Low STAT3 expression sensitizes to toxic effects of β-adrenergic receptor stimulation in peripartum cardiomyopathy

Britta Stapel[1], PhD; Michael Kohlhaas[2], PhD; Melanie Ricke-Hoch[1], PhD; Arash Haghikia[1], MD; Sergej Erschow[1], MS; Juhani Knuuti[3], MD; Johanna M. U. Silvola[3], PhD; Anne Roivainen[3], PhD; Antti Saraste, MD, PhD[3]; Alexander G. Nickel[2], PhD; Jasmin A. Saar[2], MD, PhD; Irina Gorst[1], MS; Stefan Pietzsch[1], MS; Mirco Müller[1], MD, PhD; Ivan Bogeski[4], MD; Reinhard Kappl[4], PhD, Matti Jauhiainen[5], PhD; James Thackeray[6], PhD; Michaela Scherr[7], PhD; Frank Bengel[6], MD; Christian Hagl[8], MD; Igor Tudorache[9], MD; Johann Bauersachs[1], MD; Christoph Maack[2]*, MD; and Denise Hilfiker-Kleiner[1]*, PhD

[1]Department of Cardiology and Angiology, Hannover Medical School, Hannover, Germany
[2]Clinic for Internal Medicine III, School of Medicine, Saarland University, Homburg, Germany
[3]Turku PET Centre, University of Turku and Turku University Hospital, Turku, Finland
[4]Department of Biophysics, CIPMM, School of Medicine, Saarland University, Homburg, Germany
[5]Public Health Genomics Unit, National Institute for Health and Welfare, Genomics and Biomarkers Unit, Helsinki, Finland
[6]Department of Nuclear Medicine, Hannover Medical School, Hannover, Germany
[7]Department of Hematology, Hemostasis, Oncology and Stem Cell Transplantation, Medical School Hannover, Germany
[8]Department of Cardiac Surgery, LMU, Germany
[9]Department of Cardiac, Thoracic, Transplantation and Vascular Surgery, MHH, Germany

Co-Corresponding authors:
Denise Hilfiker-Kleiner, PhD
Abt. Kardiologie und Angiologie
Medizinische Hochschule Hannover
Carl-Neuberg Str. 1
30625 Hannover, Germany
phone/fax: +49 (511) 532-2531/-3263
e-mail: hilfiker.denise@mh-hannover.de

Christoph Maack, MD
Klinik für Innere Medizin III
Universitätsklinikum des Saarlandes
66421 Homburg/Saar, Germany
Phone/fax: +49 (6841) 162-3000/-3434
Email: christoph.maack@uks.eu

Expanded Methods and Results

Patient collective

This analysis was approved by the local ethics committee of Hannover Medical School. All patients provided written informed consent and were enrolled in the German PPCM registry and were diagnosed with PPCM as described[1, 2]. Laboratory and clinical assessment such as onset of symptoms and signs during first presentation, New York Heart Association (NYHA) functional class, ECG, echocardiographic analyses, were obtained at time of diagnosis and at 8±4 months follow-up. Nonfailing samples derived from organ donors whose hearts were apparently healthy but could not be transplanted for technical reasons. For PPCM one sample derived from an explanted heart after heart transplantation and two samples were obtained at the time of LVAD implantation. The use of these tissues was approved by our local ethic committee.

Medication

Standard medication for heart failure was applied upon diagnosis and reported using beta-blocker and ACE-inhibitor/ARBs or other heart failure therapy according to the guidelines.

In addition, a healing attempt using bromocriptine therapy (BR-therapy) was present if a patient obtained bromocriptine according to the protocol published in our pilot study.[3]

Analysis of outcome

After follow-up at 8±4 months patients were classified as described previously.[1, 3, 4] In brief, patients were classified as improvers (IMP) if LVEF increased by 10 absolute percent units or if NYHA improved by one class. Patients were classified as non improvers (NIMPs) if they showed at the follow-up visit any of the parameters such as a LVEF < 35%, failed to improve LVEF by 10 absolute units, remained at a NYHA functional class of III/IV, obtained heart transplantation or an left ventricular assist device (LVAD) or had died. Full recovery was defined as reaching an LVEF of ≥ 55% and NYHA class I to II.

Animal experiments

Generation of mice with a cardiomyocyte-restricted knockout of STAT3 (*αMHC-Cre*$^{tg/+}$; *STAT3*$^{fl/fl}$, CKO) and WT littermates (*STAT3*$^{fl/fl}$) has been described previously.[5] Mice heterozygous for the *STAT3* allele were generated by crossing *αMHC-Cre*$^{tg//+}$; *STAT3*$^{fl/fl}$ mice with *STAT3*$^{fl/+}$ mice. Osmotic

minipumps were implanted subcutaneously (s.c.) under isoflurane anesthesia to infuse isoproterenol (Iso: 30 or 10 mg/kg/d), or 0.9% sodium chloride for the indicated duration. In postpartum female mice osmotic pumps were implanted between two to four days after delivery. To investigate the effect of Iso in the context of myocardial STAT3 deficiency independent of pregnancy and pregnancy hormones, sibling male mice at 10-12 weeks of age were used in the study if not indicated otherwise. Echocardiography (Vevo 770, Visual Sonics) and hemodynamic measurements (Millar cathether system, Föhr Medical Instruments) were carried out in sedated mice (isoflurane inhalation 0.5%) as described before.[6] Metoprolol tartrate (400 mg/kg/d, Sigma) and bromocriptine (4 mg/kg/d, bromocriptine mesylate, Meda) were administered by the drinking water. Perhexiline malate (25 mg/kg/d, Sigma) was dissolved in 1% methylcellulose and given orally once a day. Etomoxir (25 mg/kg/d, Calbiochem) and AST (80 mg/kg/d, Selleckchem) were injected intraperitoneally (i.p.) every 24h. 3-(3-pyridinyl)-1-(4-pyridinyl)-2-propen-1-one (3PO, 70 mg/kg/d, Calbiochem) was given by i.p. injections once a day at the first two days of Iso treatment. All interventions started immediately after implantation of minipumps.

Injection of Evans Blue dye for detection of necrotic cells

Evans Blue dye (EBD) was dissolved in 0.9 % sodium chloride (10 mg/ml) and sterile filtrated to eliminate insoluble particles. Mice received 200 µl of EBD solution once per i.p. injection 18h before they were sacrificed. Hearts were quickly excised, embedded in OCT and frozen at -80°C and thereafter cryosections were made. To determine the quantity of necrotic cardiomyocytes in the mouse myocardium, counterstaining with Fluorescein-conjugated WGA was performed to visualize cardiomyocyte plasma membranes.

Measurement of blood glucose

Blood glucose levels were determined by the use of a test strip and measurements were performed with a standard blood glucose meter (Bayer).

Measurement of serum/plasma non-esterified fatty acids (FFA)

Serum/plasma FFAs (non-esterified fatty acids) were analyzed using *in vitro* enzymatic colorimetric method (Wako Pure Chemical Industries, Ltd., Osaka, Japan). Briefly, serum/plasma FFAs were first treated with acyl-CoA synthetase (ACS) to produce acyl-CoA followed by its further transformation to

2,3-trans-Enoyl-CoA and liberation of hydrogen peroxide. The latter was then oxidatively condensed with aniline-derivative and 4-aminoantipyrine in the presence of peroxidase to generate a purple colored product that was quantified at 550 nm using EnSpire Multimode Plate Reader (PerkinElmer Inc., Waltham, USA). In practical terms, 20 µl serum/plasma was needed for the assay with a total incubation time of 20 min at 37°C.

Measurement of myocardial FFA uptake, myocardial perfusion and oxygen consumption

Myocardial perfusion and oxygen consumption, and fatty acid metabolism were assessed by [^{11}C]acetate and 14(R,S)-[^{18}F]fluoro-6-thia-heptadecanoic acid ([^{18}F]FTHA) PET using a dedicated small-animal PET scanner (Inveon, Siemens Medical Solutions Knoxville, TN, USA).

Mice were anesthetized with isoflurane (induction 3.5%, maintenance 1.5%), tail vein catheterized, placed on the scanner bed and body temperature maintained using a heating pad. To assess myocardial perfusion and oxygen consumption, a slow 11±2 MBq bolus of [^{11}C]acetate was intravenously injected via the tail vein after starting a 10 min PET acquisition. Approximately 100 min (5 times the physical half-life of [^{11}C], i.e. 20.4 min) after the [^{11}C]acetate PET, the same mice were intravenously injected with 4±2 MBq of [^{18}F]FTHA after starting a 30 min PET acquisition to assess fatty acid metabolism. Before [^{18}F]FTHA imaging, mice had fasted for 4h with *ad libitum* access to water. All PET data was acquired in three-dimensional and stored in a list-mode format.

[^{11}C]Acetate PET data was iteratively reconstructed with the ordered-subsets expectation maximization two-dimensional algorithm (OSEM2D) into 5 × 2 s, 5 × 10 s, 4 × 30 s, 7 × 60 s frames and analysed with Carimas 2.63 software (Turku PET Centre, Turku, Finland). Myocardial perfusion was determined using a single-compartment model and expressed as rate constant K_1 (1/min). Myocardial oxygen consumption was assessed by applying mono-exponential fitting to calculate [^{11}C]acetate clearance rate K_{mono} (1/min)[7]. Arterial input function was obtained from the heart left ventricle.

[^{18}F]FTHA PET data was reconstructed with OSEM3D algorithm into 5 × 2 s, 4 × 5 s, 3 × 10 s, 8 × 30 s, 5 × 60 s, 2 × 300 s, 1 × 600 s time frames and analysed with Carimas 2.63 software. The myocardial uptake of [^{18}F]FTHA was determined at 20-30 min post-injection and results were expressed as a standardized uptake value (SUV), which was calculated as the radioactivity concentration of the

region of interest divided by the relative injected radioactivity dose expressed per animal body weight, and normalized by plasma FFA level.

After the [^{18}F]FTHA PET, animals were immediately sacrificed. Under deep isoflurane anesthesia, the blood was removed by cardiac puncture followed by cervical dislocation. Samples of blood and various organs were excised, weighed, and measured for radioactivity using a gamma counter (Triathler 3", Hidex, Turku, Finland) cross-calibrated with a dose calibrator (VDC-202, Veenstra Instruments, Joure, the Netherlands). Plasma FFA level was determined as described above. Tissue uptake of [^{18}F]FTHA was expressed as SUV normalized with plasma FFA level.

Ethical statement

All animal studies were in accordance with the German animal protection law and with the European Communities Council Directive 86/609/EEC and 2010/63/EU for the protection of animals used for experimental purposes. All experiments were approved by the Local Institutional Animal Care and Research Advisory Committee and permitted by the local authority. PET imaging of [^{18}F]FTHA and [^{11}C]acetate was conducted within the Finnish Centre of Excellence in Cardiovascular and Metabolic Diseases supported by the Academy of Finland, University of Turku, Turku University Hospital and Åbo Akademi University. This study was approved by the national Animal Experiment Board (Eläinkoelautakunta, ELLA)/Regional State Administrative Agency for Southern Finland (licence number 4835/04.10.03/2011).

Functional experiments on isolated adult cardiac myocytes

Cardiomyocytes were isolated by enzymatic digestion and experiments performed as described previously[8 9]. Briefly, myocytes were electrically stimulated at 0.5 Hz and then superfused with isoproterenol (30 nM). As soon as an increase in sarcomere shortening could be observed (indicating that β-adrenoceptor activation commenced), stimulation frequency was increased to 5 Hz for 3 min and then stepped back to 0.5 Hz with isoproterenol being washed out for another minute. In the graphs of Figure 3, we show the data collected starting 1 min before stimulation was switched to 5 Hz, respectively. We collected the autofluorescence of NAD(P)H/NAD(P)$^+$ and $FADH_2$/FAD using excitation wavelengths (λ_{exc}) of 340 and 485 nm, and emission wavelengths at λ_{em} of 450 and 525 nm, respectively, as described previously[9]. To detect mitochondrial superoxide ($^{\cdot}O_2^-$), myocytes were

loaded with MitoSOX (3.3 µmol/L) for 30 min at 37°C and fluorescence excited at λ_{exc}=380 nm and emission collected at λ_{em}=580 nm. To verify specificity of the dye, antimycin A (150 µmol/L) was added at the end of every experiment and the increase in MitoSox fluorescence was determined. Only cells with a positive response to antimycin A were included in the analysis, and the increase in MitoSox fluorescence was on average not different between groups (not shown).

Mitochondria isolation

The heart was washed in ice-cold isotonic isolation solution (IS; in mM: sucrose 75, mannitol 225, HEPES 2, EGTA 1, pH 7.4) and separated from atria and non-myocardial tissue. Then the heart was transferred to a 5 ml homogenizer (Teflon pestle) and manually homogenized in two steps for 7 min each. The homogenate was centrifuged at low speed (480 x *g*, 5 min, 4°C) and the supernatant was further centrifuged (7700 x *g*, 10 min) to obtain the mitochondrial pellet and the cytosolic fraction. The pellet containing mitochondria was washed carefully twice in 1.4 ml mitochondrial suspension solution (MSS; like IS, but without EGTA), centrifuged (7700 x *g*, 5 min), and finally resuspended in 100 µl of MSS. Mitochondrial protein concentrations were determined according to the method of Lowry.

Mitochondrial respiration measurements

Oxygen (O_2) consumption was measured polarographically in 400 µg of cardiac mitochondria respiring on pyruvate/malate (5 mM, respectively) at 30°C with a Clark oxygen electrode (Hansatech) covered with an ultrathin Teflon membrane in a closed chamber (Hansatech, oxygraph) of 2 ml containing (in mM) KCl 137, KH_2PO_4 2, EGTA 0.5, $MgCl_2$ 2.5, HEPES 20, at pH 7.2. State 2 respiration was initiated by the addition of pyruvate/malate, while state 3 respiration was induced by the addition of ADP (1 mM) after 3 and 4.5 min, respectively. Subsequent addition of the F_1F_o ATP-synthase inhibitor oligomycin (1.2 µM) induced State 4 respiration, which did not differ from State 2 respiration in all groups.

EPR spin trap

Detection of $^{\cdot}O_2^-$ production in isolated mitochondria was performed by electron paramagnetic resonance (EPR) analysis using the redox activated cyclic hydroxylamine spin trap CMH (1-hydroxy-3-methoxycarbonyl-2,2,5,5-tetramethylpyrrolidine; 300 µM) as described previously[9]. Experiments

were performed with a Bruker spectrometer (ESP300e) equipped with a standard 4102ST cavity, which holds the capillary support quartz glass finger. The finger is temperature-controlled and set to 37°C. The redox activated cyclic hydroxylamine spin trap CMH (1-hydroxy-3-methoxycarbonyl-2,2,5,5-tetramethylpyrrolidine; 300 µM) was used for all experiments to monitor superoxide ($^{\cdot}O_2^-$) production. CMH was added shortly before the experiment. The sample was filled in a 50 µl glass capillary and immediately transferred into the capillary holder. All control experiments with single components of the assays and CMH were tested for unspecific radical production.

The EPR spectra of the CM radical were measured with modulation amplitude of 0.1 mT and a microwave power of 20 mW at a time constant of 20.48 ms for 8 times and evaluated with a customized program (Medeia) which determines the peak-to-peak intensity and width of one (or several) lines of a radical visible in a time series. In the absence of line width changes and saturation effects, the intensity information can be translated to radical concentration by calculating the integral of the monitored line and considering the multiplicity of the radical signal. This value is compared to a reference sample of known concentration (100 µM TEMPOL) recorded under identical conditions for quantitative measures.

H_2O_2 emission

H_2O_2 emission from mitochondria was measured using the H_2O_2-sensitive and specific fluorescent dye Amplex®UltraRed (AUR; life technologies, Molecular Probes®). AUR reacts with H_2O_2 to form fluorescent product Resorufin (excitation at 535 nm, emission at 590 nm) in a 1:1 relation. The reaction is catalyzed by horseradish peroxidase (HRP). Assay component concentrations were 50 µM for AUR, 0.5 U/ml for HRP and 100 U/ml SOD (for conversion of O_2^- to H_2O_2). Mitochondrial H_2O_2 production was measured after treatment with ADP (1 mM), FCCP (5 µM) and antimycin A (15 µM) in the presence of pyruvate/malate (5 mM), respectively, or mitochondria alone. Experiments were performed in 96-well plates (black/transparent) using the Tecan GENios Pro Reader with a bottom reading setting. All experiments were conducted in respiration buffer with 30 µg mitochondria per well in triplicates at 37°C. H_2O_2 was quantified from a calibration curve obtained from known H_2O_2 concentrations.

Triglyceride, pyruvate and lactate content

For measurement of triglyceride, pyruvate and lactate content commercially available assay kits (Abcam) were used in accordance to the manufacurer's protocol and values were normalized to protein content.

ADP/ATP ratio

ADP/ATP ratio was analyzed using a commercially available kit (ADP/ATP Ratio Assay Kit (Bioluminescent), Abcam) with slight changes to the manufacture's protocol as follows. Hearts were excised and tissue was snap frozen in liquid N_2. LV tissue samples were weighted and rapidly homogenized on ice in Nucleotide Releasing Buffer (10 mg in 100 µl). Samples were centrifuged for 2 min at 14.000 x g and 4°C to exclude cell debris and supernatants were diluted 1:30 in Nucleotide Releasing Buffer on ice. 100 µl of each sample were transferred onto a 96-well luminometer plate in dublicates. Ten µl ATP Monitoring Enzyme was added to each well and luminescence was recorded a minute later (Data A). The plate was incubated at room temperature and protected from light for 10 min before luminescence was measured again (Data B). Ten µl ADP Converting Enzyme was added to each well and luminescence was recorded after 1 min (Data C). ADP/ATP ratio was calculated as (Data C - Data B)/Data A.

Histology and immunostaining

For analysis of LV dimensions, hearts were fixed *in situ*, embedded in paraffin, and stained with H&E, as described [5]. Interstitial collagen volume fraction was determined in picro-Sirius red-stained LV cryosections [5]. Mean cardiomyocyte cross-sectional area (CSA) and cardiomyocyte length (CML) were determined in *in situ* fixed sections stained with wheat germ agglutinin (WGA, Vector) [10, 11]. Inflammation was determined in LV cryosections with antibodies recognizing CD45 (BD Pharmingen, Clone 30-F11) [10, 11]. GLUT4 immunostaining was performed (GLUT4, 1:100, Abcam, ab654) to determine GLUT4 expression and localization. STAT3 protein in human LV samples was detected by immunohistochemistry on frozen sections after acetone fixation and permeabilization with methanol using mAB against STAT3 (CST, 9139) with the DAB method. For nuclear staining DAPI, Hoechst 33258 (Sigma) or haematoxyline was used.

qRT-PCR, miR-qRT-PCR, Western blot

Total RNA from adult murine hearts was isolated with Trizol (Invitrogen) and cDNA synthesis was performed as described previously [10, 11]. Realtime PCR using the SYBR green dye method (Brilliant SYBR Green Mastermix-Kit, Stratagene) was performed with the Stratagene MX3005P multiplex QPCR System as described [10, 11]. Expression of mature miR-7a (Applied BioSystems) was determined using miR-qRT-PCR on an ABI7500 cycler (Applied Biosystems, Foster City, USA) and was normalized using the 2-ΔΔCT method relative to U6 as described [12].

Protein expression levels were determined by Western blotting, using SDS-PAGE as previously described [5]. The following antibodies were used: anti-STAT3 mAb (CST, 9139 and 4904), anti-HER2/ErbB2 mAb (CST, 4290), anti-HER4/ErbB4 mAB (CST, 4795), anti-GAPDH mAb (CST, 2118), anti-phospho-TnI S23/24 pAb (CST, 4004), anti-TnI pAb (CST, 4002) anti-GLUT1 pAb (Abcam, ab652), anti-GLUT4 pAb (Abcam, ab654), anti-phospho-ADAM17 T735 pAb (Abcam, ab182630), anti-ADAM17 pAb (Abcam, ab2051) and anti-VDAC1 pAb (Santa Cruz sc-32063). Secondary HRP-conjugated, anti-rabbit, anti-goat or anti-mouse Ab (Amersham) were used.

Experiments with neonatal rat cardiomyocytes (NRCM)

Isolation of NRCM and cultivation in DMEM high glucose 4.5 g/L and M199 (4:1) was described previously [13].

SiRNA-mediated knockdown of ErbB4 was performed by transfection of a pool of four specific siRNAs (Dharmacon Research Inc) at a final concentration of 25 nM using Dharmafect-1 (Dharmacon Research Inc) transfection reagent in accordance to the manufacturer's instructions and analyses were carried out 4d after transfection.

Overexpression of miR-199a was achieved by adenoviral transduction using an adenoviral vector system (Quantum Appligene) as previously reported [14], containing a miR-199a construct as described before [13].

MiR-7a was overexpressed by transfection with pre-miR-7a (100 nM, Ambion) using lipofectamin (Invitrogen) in accordance to the manufacture's instruction.

Glucose uptake of NRCM was assessed after cells were starved for 2 h in glucose-free DMEM/M199 medium (4:1) by addition of [^{18}F]FDG (250 kBq/mL) with or without insulin (50 nM, Lilly) or NRG1 (14 nM, Immunotools). After 60 min incubation at 37°C, residual medium was removed, cells were

washed twice with 1 mL warm glucose-free medium, and lysed in RIPA buffer. Lysates were counted in a gamma counter along with a 1% dilution of the standard injection. Radioactivity was normalized to total protein content in lysates.

Metabolic activity was analyzed using a tetrazolium-based (MTT) assay (Promega).

Hyperosmolar conditions were achived by addition of 100 mM NaCl to FBS-free culture medium for 24 h.

Modulation of miR-199a expression and immunoprecipitation of Human Argonaute 2 Complexes with the RIP kit

In silico analyses were performed using TargetScan[15] and/or RNA22[16].

NRCM were transfected with pre-miR-199a or an antagomir against miR-199a (100 nM, Ambion). Cells were lysed in RIP-lysis buffer 5d after transfection. MicroRNA:mRNA immunoprecipitation was performed using the Magna RIP kit (Millipore) following the manufacturer's protocol as previously described [12]. Briefly, for RISC-IPs of NRCM, $1x10^7$ cells were taken for each replicate, washed in PBS before lysis in 100 µl complete RIP-lysis buffer and incubated with magnetic beads conjugated with anti-Ago2/eIF2C2 antibody and rotated overnight at 10°C. Co-immunoprecipitated RNA, including miRNA:mRNA complexes was subjected to qRT-PCR and miR-qRT-PCR. Expression of mature miRNAs was determined by miR-qRT-PCR using miRNA-specific looped RT-primers and TaqMan probes as recommended by the manufacturer (Applied Biosystems). Normalization was performed using the 2-ΔΔCT method relative to U6snRNA.

Sequences of qRT-PCR primers

mRNA	Sense primers (5' to 3')	Antisense primers (5' to 3')
mmu 18S	GTAACCCGTTGAACCCCATT	CCATCCAATCGGTAGTAGCG
mmu ANP	GCCGGTAGAAGATGAGGTCA	GGGCTCCAATCCTGTCAATC
mmu BNP	AAGAGAAAAGTCGGAGGAAAT	CTTCAGTGCGTTACAGCCC
mmu/rno B2M	CATGGCTCGCTCGGTGACC	AATGTGAGGCGGGTGGAACTG

mmu ErbB4	GTGCTATGGACCCTACGTTAGT	TCATTGAAGTTCATGCAGGCAA
rno ErbB4	GTGCTATGGACCCTACGTCAGT	TCATTGAAGTTCATGCAGGCAA
mmu GLUT4	AAACAAGATGCCGTCGGGT	ATAGCCAAACTGAAGGGAGCC

Statistical analysis for patient data

Database management and statistical analyses were performed with PRISM software version 5.0a and SPSS version 22. Continuous data were expressed as mean±SD, median and range or proportions. Comparison of means between patients' treatment groups at baseline was performed by unpaired t-test after testing for normal distribution using the Kolmogorov–Smirnov test and comparison of proportions was performed by Fisher exact test, respectively. Significance was assumed at a two-sided value of $P<0.05$.

Statistical analyses for experimental models

Statistic analysis was performed using Microsoft® Excel® or GraphPad Prism 6 software. All data were considered to be normally distributed and analysis was carried out using two-tailed Student's t-test (within the test oft he manuscript indicated as #P) or two-way ANOVA followed by Bonferroni post-hoc test (within the text of the manuscript indicated as *P) as indicated. Survival data were analysed using Log-rank (Mantel-Cox) test. Differences were considered as statically significant for $P<0.05$. All data are depicted as mean ±SD as indicated.

Supplemental Results

An anti-Argonaute (AGO) ribonucleoprotein immunoprecipitation (RIP) assay revealed increased ErbB4 mRNA (1.6-fold) in the AGO-containing microribonucleoprotein (miRNP) effector complex precipitated from NRCM transfected with pre-miR-199a when compared to antagomir-transfected cells, indicating that ErbB4 is a direct target of miR-199a.

Supplemental Figures

Online Figure I

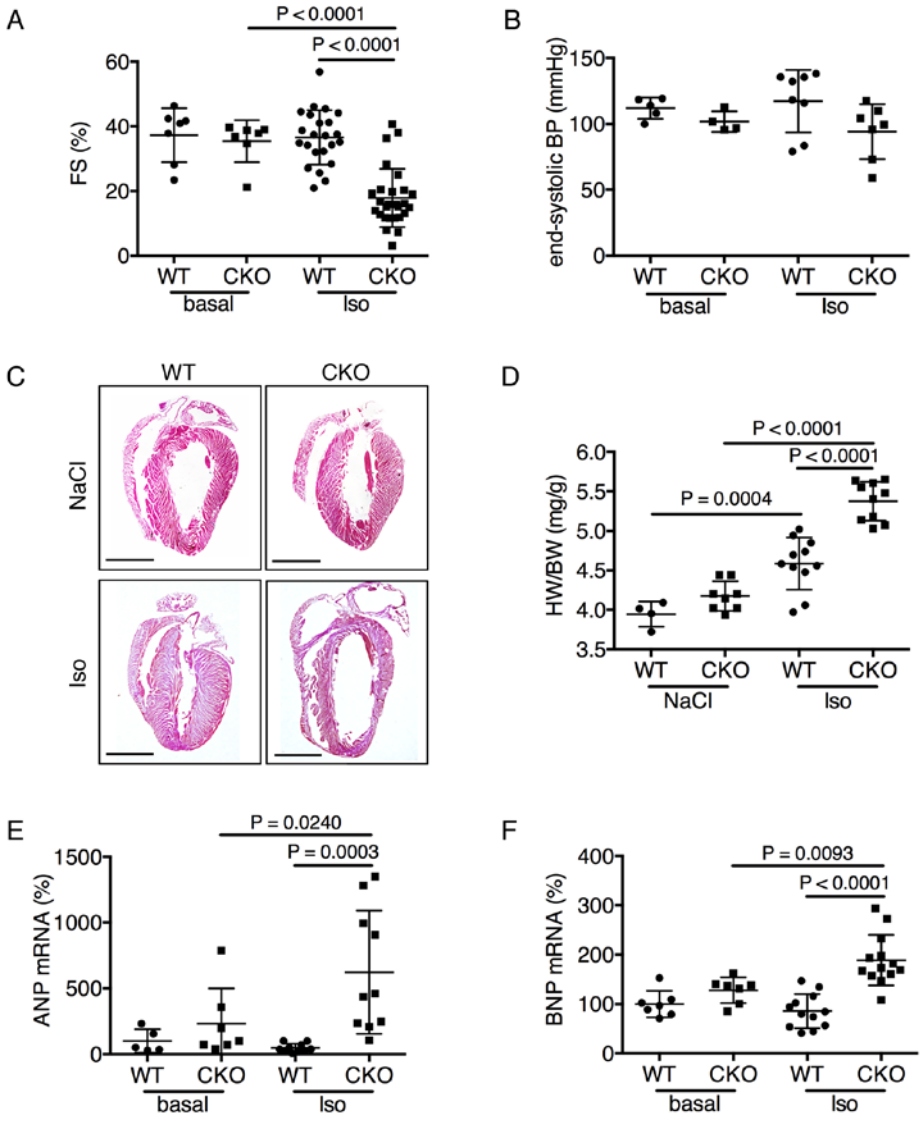

Online Figure I: (**A**) Systolic LV function (fractional shortening; %FS) in WT and CKO mice after 14d NaCl- or Iso-stimulation (n=7-29). (B) Invasive measurements of end-systolic blood pressure (BP) of WT and CKO mice after 14d of NaCl- or Iso-treatment (n=4-9) assessed by Millar catheter. **C**) Representative pictures of in *situ fixed*, H&E stained longitudinal cardiac sections (scale bars: 4 mm) and (**D**) heart weight (HW) to body weight (BW) ratio of NaCl- or Iso-treated WT and CKO mice (n=4-17). (**E**) ANP or (**F**) BNP mRNA levels (qRT-PCR) in WT and CKO hearts, basal and 3d

of Iso treatment (WT basal set 100%; n=5-13). Data are presented as means±SD. *P*-values were evaluated by two-way ANOVA followed by Bonferroni post-hoc test.

Online Figure II

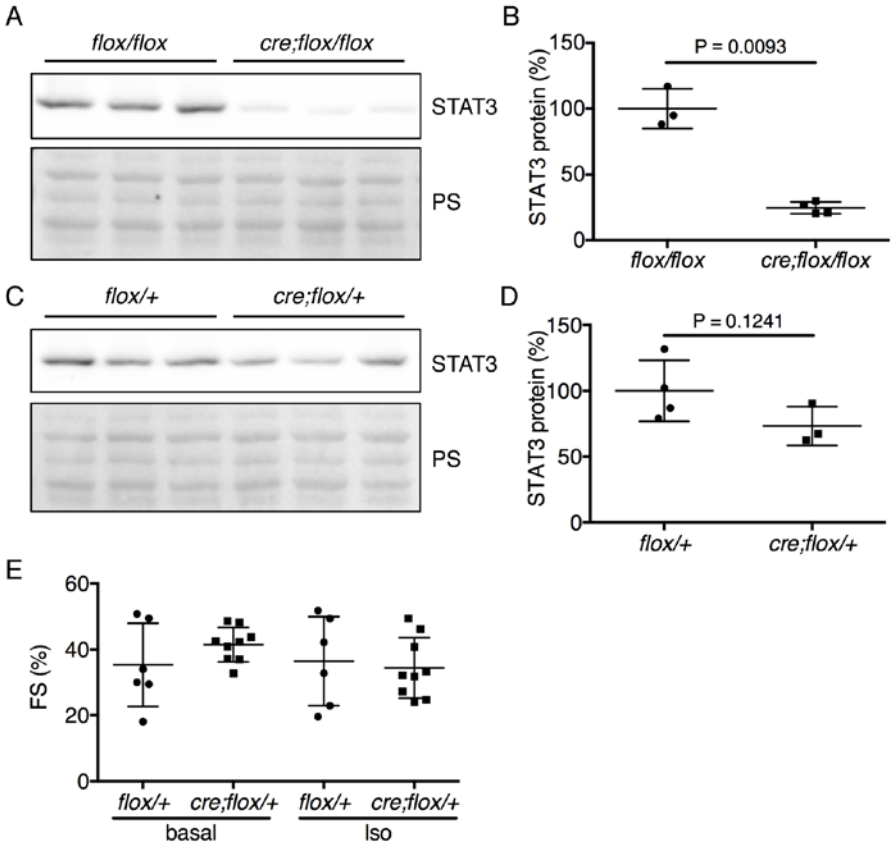

Online Figure II: (**A)** Western blot of LV STAT3 protein and (**B**) quantification of STAT3 protein levels in WT (*flox/flox*) and CKO (*cre;flox/flox*) mice at baseline (WT set as 100%; n=3-4). (**C**) Western blot of LV STAT3 protein and (**D**) quantification in WT (*flox/+*) and heterozygous (*cre;flox/+*) LV (WT set as 100%; n=3-4). (**E**) LV function (fractional shortening; %FS) of WT and mice heterozygous for STAT3 at baseline and after 14d of Iso-treatment (n=6-9). For (A-E): All data are means±SD. *P*-values were computed by two-tailed Student's t-test.

Online Figure III

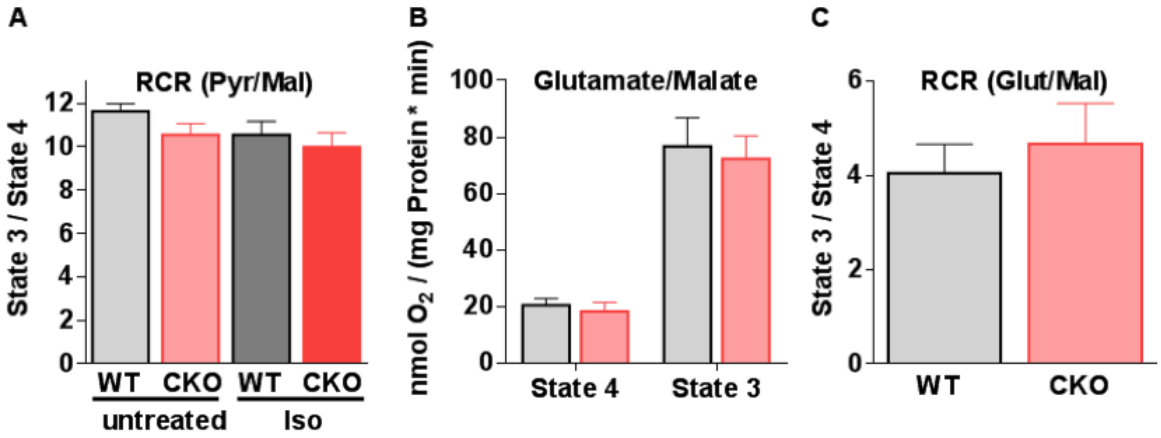

Online Figure III: (**A**) Respiratory control ratios (State 3/State 4 respiration) in isolated mitochondria respiring on pyruvate/malate from untreated or Iso-treated (conc.) CKO or WT mice, respectively (n=6-7). Respiration in the absence (State 4) and presence (State 3) of ATP in isolated mitochondria of CKO and WT mice respiring on glutamate/malate (**B**), and the respiratory control ratio calculated from these data (**C**). Untreated: WT, n=6; CKO, n=9; Iso-treated: WT, n=8; CKO, n=8. All data are means±SD. *P*-values were calculated by two-tailed Student's t-test.

Online Figure IV

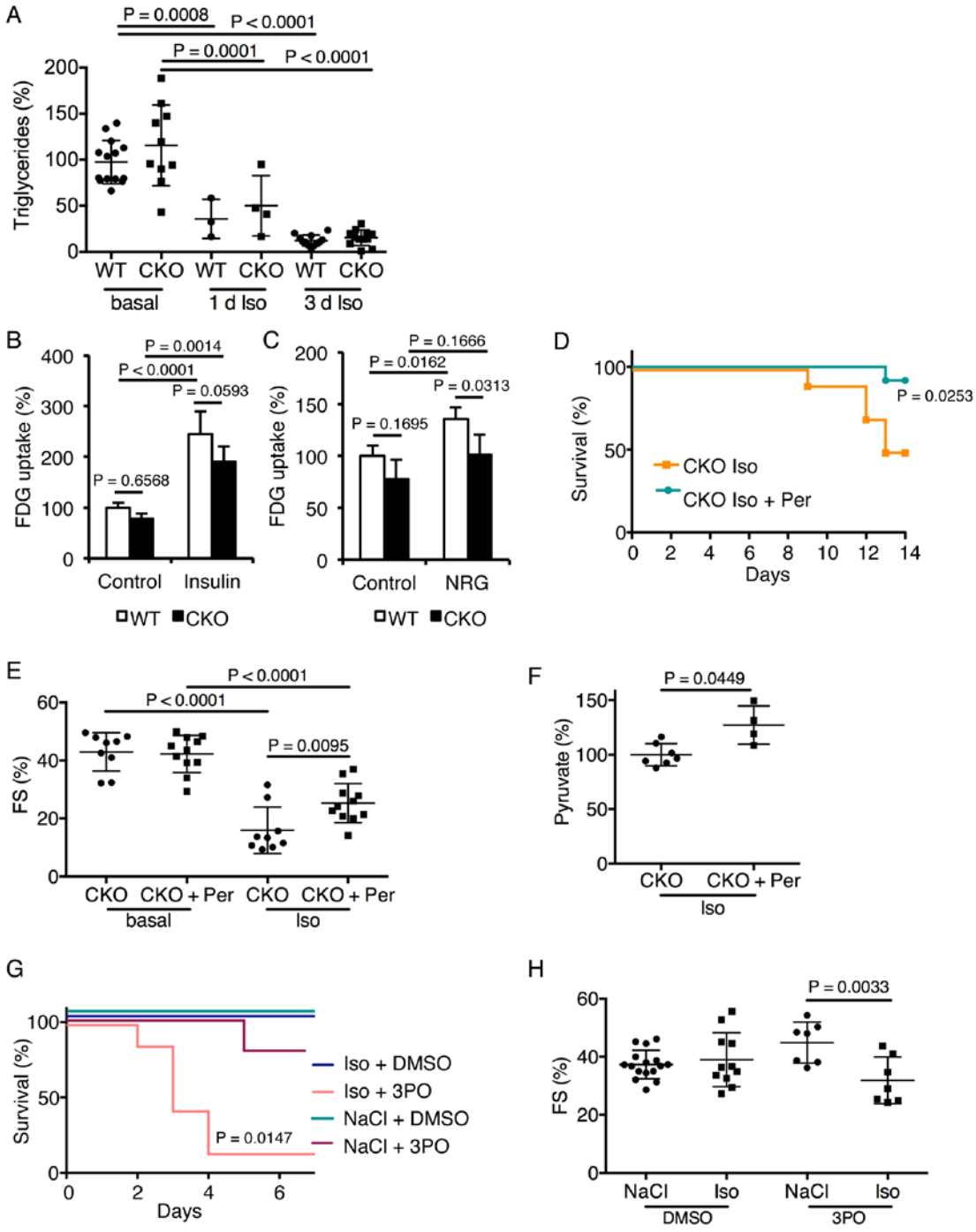

Online Figure IV: (A) Quantification of triglyceride content in LV tissue samples of WT and CKO hearts at baseline, after 1d and after 3d of Iso-treatment (n=3-14). [^{18}F]FDG uptake in adult cardiomyocytes isolated from WT or CKO hearts at baseline after acute stimulation with insulin (50 nM, **B**) or neuregulin 1 (NRG, 14 nM, **C**) (n=3-4 animals per group). (**D**) Kaplan-Meier curve depicting survival proportions after 14d (n=10-12) and (**E**) LV function (%FS, n=9-11) after 7d of CKO mice treated with Iso alone or co-treated with perhexiline (Per, 25 mg/kg/d). (**F**) Quantification

of pyruvate content in LV samples of CKO mice treated with Iso or with Iso and perhexiline (Per, 25mg/kg/d) for 3d (n=4-7). **(G)** Kaplan-Meier survival analysis over 7d and (**H**) LV function (%FS) after 3d in WT mice treated with PFKFB3-inhibitor 3PO (70 mg/kg/d) alone or in combination with Iso or saline (n=5-7). All data are means±SD. Survival curves were analysed using Log-rank (Mantel-Cox) test. *P*-values were assessed by two-way ANOVA and Bonferroni post-hoc test (**A, B, C, E and H** or by two-tailed Student's t-test (**E**).

Online Figure V

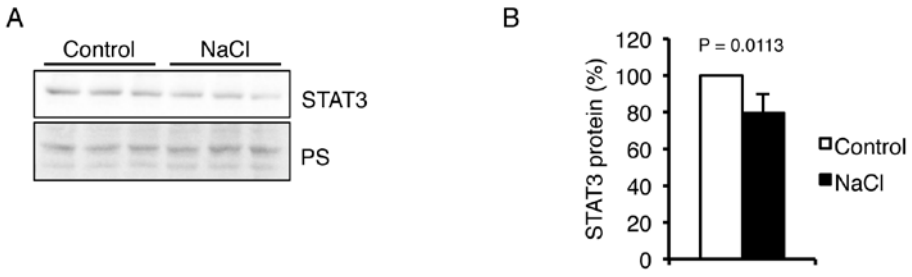

Online Figure V: (**A**) Western blot depicting STAT3 protein in NRCM after 24h culture in hyperosmolar conditions (100 mM NaCl) compared to control cells and (**B**) quantification of STAT3 protein normalized to Ponceau S (PS). Data are means±SD. *P*-values were assessed by two-tailed Student's t-test. Experiments were performed in five independent cell preparations in at least triplicates.

References

1. Haghikia A, Podewski E, Libhaber E, Labidi S, Fischer D, Roentgen P, Tsikas D, Jordan J, Lichtinghagen R, von Kaisenberg CS, Struman I, Bovy N, Sliwa K, Bauersachs J, Hilfiker-Kleiner D. Phenotyping and outcome on contemporary management in a German cohort of patients with peripartum cardiomyopathy. Basic Res Cardiol 2013;**108**(4):366.
2. Sliwa K, Hilfiker-Kleiner D, Petrie MC, Mebazaa A, Pieske B, Buchmann E, Regitz-Zagrosek V, Schaufelberger M, Tavazzi L, van Veldhuisen DJ, Watkins H, Shah AJ, Seferovic PM, Elkayam U, Pankuweit S, Papp Z, Mouquet F, McMurray JJ. Current state of knowledge on aetiology, diagnosis, management, and therapy of peripartum cardiomyopathy: a position statement from the Heart Failure Association of the European Society of Cardiology Working Group on peripartum cardiomyopathy. Eur J Heart Fail 2010;**12**(8):767-78.
3. Sliwa K, Blauwet L, Tibazarwa K, Libhaber E, Smedema JP, Becker A, McMurray J, Yamac H, Labidi S, Struman I, Hilfiker-Kleiner D. Evaluation of bromocriptine in the treatment of acute severe peripartum cardiomyopathy: a proof-of-concept pilot study. Circulation 2010;**121**(13):1465-73.
4. Sliwa K, Forster O, Tibazarwa K, Libhaber E, Becker A, Yip A, Hilfiker-Kleiner D. Long-term outcome of peripartum cardiomyopathy in a population with high seropositivity for human immunodeficiency virus. Int J Cardiol 2011;**147**(2):202-8.
5. Hilfiker-Kleiner D, Hilfiker A, Fuchs M, Kaminski K, Schaefer A, Schieffer B, Hillmer A, Schmiedl A, Ding Z, Podewski E, Poli V, Schneider MD, Schulz R, Park JK, Wollert KC, Drexler H. Signal transducer and activator of transcription 3 is required for myocardial capillary growth, control of interstitial matrix deposition, and heart protection from ischemic injury. Circ Res 2004;**95**(2):187-95.
6. Hilfiker-Kleiner D, Kaminski K, Podewski E, Bonda T, Schaefer A, Sliwa K, Forster O, Quint A, Landmesser U, Doerries C, Luchtefeld M, Poli V, Schneider MD, Balligand JL, Desjardins F, Ansari A, Struman I, Nguyen NQ, Zschemisch NH, Klein G, Heusch G, Schulz R, Hilfiker A, Drexler H. A Cathepsin D-Cleaved 16 kDa Form of Prolactin Mediates Postpartum Cardiomyopathy. Cell 2007;**128**(3):589-600.
7. Kivela R, Bry M, Robciuc MR, Rasanen M, Taavitsainen M, Silvola JM, Saraste A, Hulmi JJ, Anisimov A, Mayranpaa MI, Lindeman JH, Eklund L, Hellberg S, Hlushchuk R, Zhuang ZW, Simons M, Djonov V, Knuuti J, Mervaala E, Alitalo K. VEGF-B-induced vascular growth leads to metabolic reprogramming and ischemia resistance in the heart. EMBO Mol Med 2014;**6**(3):307-21.
8. Chen Y, Csordas G, Jowdy C, Schneider TG, Csordas N, Wang W, Liu Y, Kohlhaas M, Meiser M, Bergem S, Nerbonne JM, Dorn GW, 2nd, Maack C. Mitofusin 2-containing mitochondrial-reticular microdomains direct rapid cardiomyocyte bioenergetic responses via interorganelle Ca(2+) crosstalk. Circ Res 2012;**111**(7):863-75.
9. Nickel AG, von Hardenberg A, Hohl M, Loffler JR, Kohlhaas M, Becker J, Reil JC, Kazakov A, Bonnekoh J, Stadelmaier M, Puhl SL, Wagner M, Bogeski I, Cortassa S, Kappl R, Pasieka B, Lafontaine M, Lancaster CR, Blacker TS, Hall AR, Duchen MR, Kastner L, Lipp P, Zeller T, Muller C, Knopp A, Laufs U, Bohm M, Hoth M, Maack C. Reversal of Mitochondrial Transhydrogenase Causes Oxidative Stress in Heart Failure. Cell Metab 2015;**22**(3):472-84.
10. Hilfiker-Kleiner D, Shukla P, Klein G, Schaefer A, Stapel B, Hoch M, Muller W, Scherr M, Theilmeier G, Ernst M, Hilfiker A, Drexler H. Continuous glycoprotein-130-mediated signal transducer and activator of transcription-3 activation promotes inflammation, left ventricular rupture, and adverse outcome in subacute myocardial infarction. Circulation 2010;**122**(2):145-55.
11. Hoch M, Fischer P, Stapel B, Missol-Kolka E, Sekkali B, Scherr M, Favret F, Braun T, Eder M, Schuster-Gossler K, Gossler A, Hilfiker A, Balligand JL, Drexler H, Hilfiker-Kleiner D. Erythropoietin preserves the endothelial differentiation capacity of cardiac progenitor cells and reduces heart failure during anticancer therapies. Cell Stem Cell 2011;**9**(2):131-43.
12. Halkein J, Tabruyn SP, Ricke-Hoch M, Haghikia A, Nguyen NQ, Scherr M, Castermans K, Malvaux L, Lambert V, Thiry M, Sliwa K, Noel A, Martial JA, Hilfiker-Kleiner D, Struman I. MicroRNA-146a is a therapeutic target and biomarker for peripartum cardiomyopathy. J Clin Invest 2013;**123**(5):2143-54.
13. Haghikia A, Missol-Kolka E, Tsikas D, Venturini L, Brundiers S, Castoldi M, Muckenthaler MU, Eder M, Stapel B, Thum T, Petrasch-Parwez E, Drexler H, Hilfiker-Kleiner D, Scherr M. Signal transducer and activator of transcription 3-mediated regulation of miR-199a-5p links cardiomyocyte

and endothelial cell function in the heart: a key role for ubiquitin-conjugating enzymes. Eur Heart J 2011;**32**(10):1287-97.
14. Hilfiker-Kleiner D, Hilfiker A, Castellazzi M, Wollert KC, Trautwein C, Schunkert H, Drexler H. JunD attenuates phenylephrine-mediated cardiomyocyte hypertrophy by negatively regulating AP-1 transcriptional activity. Cardiovasc Res 2006;**71**(1):108-17.
15. Friedman RC, Farh KK, Burge CB, Bartel DP. Most mammalian mRNAs are conserved targets of microRNAs. Genome Res 2009;**19**(1):92-105.
16. Miranda KC, Huynh T, Tay Y, Ang YS, Tam WL, Thomson AM, Lim B, Rigoutsos I. A pattern-based method for the identification of MicroRNA binding sites and their corresponding heteroduplexes. Cell 2006;**126**(6):1203-17.